İleri Teknoloji Bilimleri Dergisi
Journal of Advanced Technology Sciences
ISSN:2147-3455

A BIDIRECTIONAL 3-INPUT DC-DC CONVERTER FOR ELECTRICAL VEHICLES

Fürkan Akar

Düzce Üniversitesi, Teknoloji Fakültesi, Elektrik-Elektronik Mühendisliği Bölümü
furkanakar@duzce.edu.tr

Abstract- In this paper, a bidirectional multi-input converter having 3 inputs for electric vehicles is investigated. In order to respond high power need of an electric vehicle during acceleration, the studied converter has the capability of transferring source energies to the output simultaneously by allowing active control of their power levels. It also enables energy transfer between sources to store redundant power or so as to avoid undercharge and overcharge conditions. Moreover, thanks to its bidirectional operation capability, it is also possible to store regenerative braking energy to input sources while keeping energy flow between these sources possible. After giving the deep analysis of the converter operation modes, the converter is simulated through a switching model in order to verify the analysis.

Key Words- Bidirectional, Electric Vehicles, Hybrid Systems, Multi-Input Converters.

ELEKTRİKLİ ARAÇLAR İÇİN ÇİFT YÖNLÜ 3 GİRİŞLİ BİR DC-DC DÖNÜŞTÜRÜCÜNÜN ANALİZİ

Özet- Bu çalışmada elektrikli araçlarda kullanılabilecek 3 girişe sahip çok girişli bir dönüştürücü ayrıntılı bir şekilde incelenmektedir. Giriş kaynaklarının enerjilerini aktif güç kontrolü yaparak yüke aktarabilen bu dönüştürücü, elektrikli araçların hızlanma anlarındaki yüksek güç talebine cevap verebilme yeteneğine sahiptir. Ayrıca, kaynaklar arasında da enerji akışı sağlanabilmekte, böylelikle fazla enerjinin saklanması ile kaynak gerilimlerinin istenilen seviyelerde tutulabilmesi mümkün olabilmektedir. Kaynaklar arasındaki enerji akışına olanak sağlamaya devam ederken, çift yönlü çalışabilmesi sayesinde, bu dönüştürücü faydalı frenleme enerjisini de kaynaklara aktarabilmektedir. Adı geçen çalışma modlarının ayrıntılı analizinden sonra, bu analiz simülasyon ortamında bir anahtarlama modeli ile doğrulanmıştır.

Anahtar Kelimeler- Çift Yönlü, Çok Girişli Dönüştürücü, Elektrikli Araçlar, Hibrit Sistemler.

1. INTRODUCTION (GİRİŞ)

It is known that excessive usage of fossil fuels makes a great contribution to the global warming. Therefore, studying on electric vehicles that utilize alternative energy sources and increasing their penetration to the transportation system can strengthen our hands to fight against global warming [1]. Among these electric vehicles, battery electric vehicles, fuel cell (FC) electric vehicles, and solar (PV) electric vehicles having photovoltaic (PV) systems have been comprehensively studied in the literature. However, the number of commercial electric

vehicles is still limited since they suffer from several drawbacks, such as, low power density, long charging time, short driving range, high cost, etc [2]. In order to overcome these drawbacks, constructing hybrid systems concept is proposed [3]. Hybridization of these energy sources not only eliminate the aforementioned drawbacks but also combines powerful features of energy sources and energy storage elements. For building hybrid systems, researchers have proposed passive hybridization techniques and several power electronics based solutions; for example, separate converters are utilized in [4] for a FC/battery/ultra-capacitor (UC) vehicular system, and a multi-input converter (MIC) is used in [5] to build a PV/FC/battery power system. MICs are known for their low cost, full power control ability, high energy density, and control simplicity in comparison to other two methods [5]. In [6] and [7], a MIC is offered and analyzed for 2-input case, then via a battery/UC hybrid energy storage system, its feasibility is verified. However, energy transfer between its sources and 3-input case are neither analyzed nor realized. Therefore, this study offers a deep analysis of this converter when it has 3 inputs. All possible operation modes are introduced and typical waveforms in these modes are given. Combining sources with different electrical characteristics and terminal voltages, this converter can easily enable to build hybrid systems like battery/ UC in [8], FC/UC in [9], PV/UC/battery in [10], and FC/battery/UC in [11].

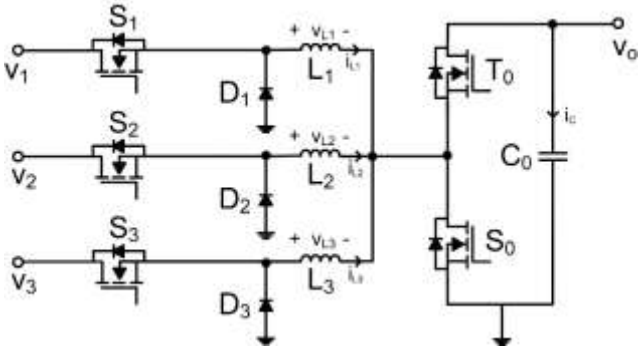

Figure 1.1. 3-input bidirectional converter. (3 girişli çift yönlü dönüştürücü)

The studied converter in this work is illustrated in Figure 1.1. As can be seen, it has 5 active switches, 3 diodes, 3 inductors and one output capacitor. It can operate in buck and boost modes when transferring energy to the output while it can operate in buck mode when transferring energy from the output. S_1, S_2, S_3, S_0, and T_0 switches are controlled by pulse-width-modulation (PWM) with d_{S1}, d_{S2}, d_{S3}, d_{S0}, and d_{T0} duty cycles, respectively. Inductors, L_1, L_2, and L_3 allow bidirectional energy transfer and diodes D_1, D_2, and D_3 carry inductors currents, i_{L1}, i_{L2}, and i_{L3}, when the associated switch is OFF. Output capacitor, C_0, charge or discharge and its current i_C becomes positive or negative according to the operation mode of the converter. Note that even though it is possible to increase the input sources, this work focuses on 3-input case.

2. METHOD (YÖNTEM)

The proposed converter has four different operation modes as given in Figure 1.2. In Mode 1A and Mode 1B, sources feed the output while in Mode 2A and Mode 2B, sources are fed by regenerative braking energy. In the analysis, the converter is composed of ideal elements and its inductor works in continuous conduction mode (CCM). Moreover, it is assumed that $V_1>V_0>V_2>V_3$ where V_1, V_2, and V_3 are source voltages and V_0 is the output voltage.

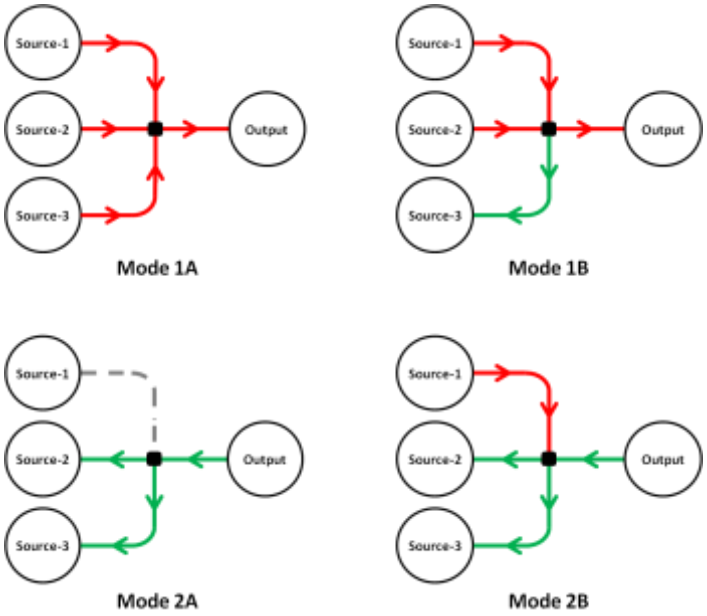

Figure 2.1. Converter operation modes. (Dönüştürücü çalışma modları)

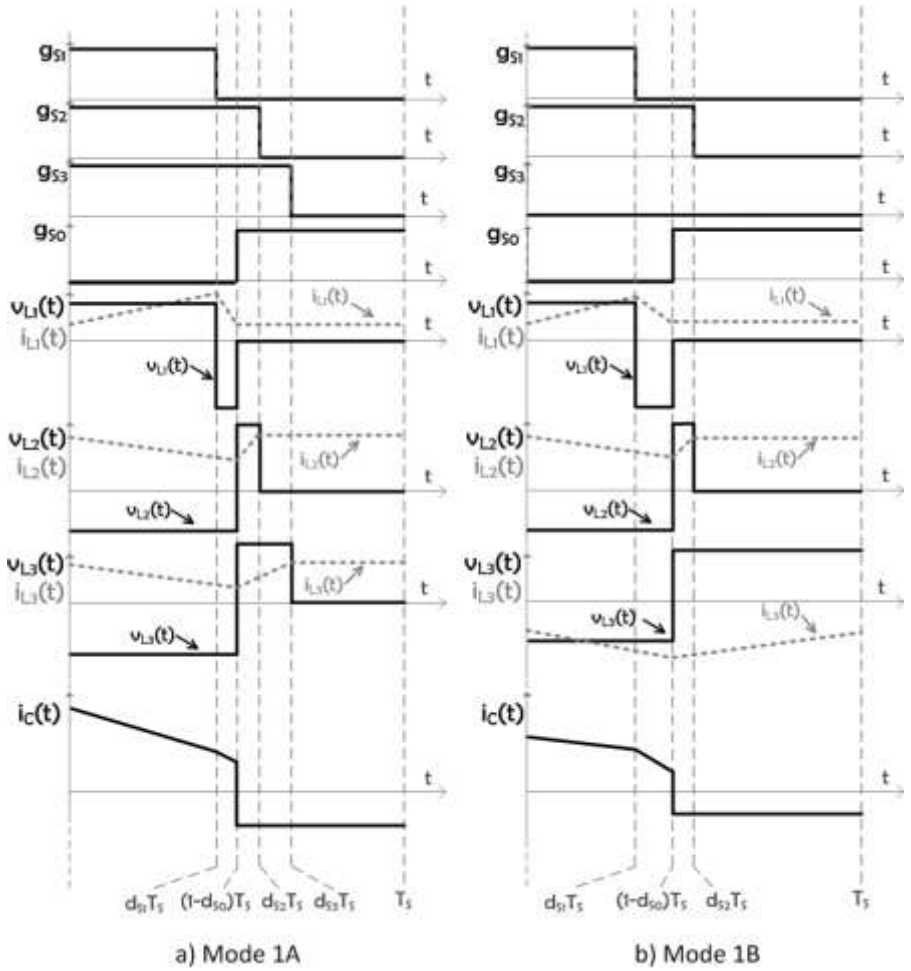

Figure 2.2. Waveforms for Mode 1A and Mode 1B. (Mode 1A ve Mode 1B için dalga şekileri)

2.1. Mode 1A

In this mode, all sources transfer their energies to the output. Therefore, all inductor currents are positive. Mode 1A consists of five switching subintervals as illustrated in Figure 2.2a.

Subinterval 1 [$0<t<d_{s1}T_s$]: At t=0 S_1, S_2, and S_3 are closed while S_0 is opened. In this period, i_{L1} is increasing due to the positive voltage across L_1. Conversely, i_{L2} and i_{L3} are decreasing since negative voltages appear across L_2 and L_3. In addition, the output capacitor is charged by positive inductor currents.

Subinterval 2 [$d_{s1}T_s <t<(1- d_{s0}) T_s$]: At $t=d_{s1}T_s$, S_1 is turned OFF while S_2 and S_3 are still kept closed. Hence, i_{L1} starts to decrease like i_{L2} and i_{L3} because the voltage across L_1 also becomes negative. Moreover, the output capacitor continues to be charged.

Subinterval 3 [$(1- d_{s0}) T_s <t< d_{s2}T_s$]: This interval starts by turning ON S_0 at $t=(1- d_{s0}) T_s$. In this period, i_{L1} becomes constant due to the freewheeling while i_{L2} and i_{L3} are increased by positive voltages across L_2 and L_3. Turning ON S_0 also initiates the discharging of the output capacitor to feed the load.

Subinterval 4 [$d_{s2}T_s <t< d_{s3}T_s$]: At $t= d_{s2}T_s$, S_2 is turned OFF and freewheeling of i_{L2} also starts. Moreover, i_{L3} is still increasing and the output capacitor is still discharging.

Subinterval 5 [$d_{s3}T_s <t< T_s$]: Turning of S_3 starts the last switching subinterval of Mode1A. Like i_{L1} and i_{L2}, i_{L3} becomes also constant since the voltage across L_3 is zero in this period. Furthermore, the output capacitor goes on the feed the load.

After completing the analysis of switching subintervals, equations summarizing the inductor voltage variations can be written as follows:

$$v_{L1}(t)=\begin{cases} V_1-V_0, & 0<t<d_{S1}T_s \\ -V_0, & d_{S1}T<t<(1-d_{S0})T_s \\ 0, & (1-d_{S0})T_s<t<T_s \end{cases} \tag{2.1}$$

$$v_{L2}(t)=\begin{cases} V_2-V_0, & 0<t<(1-d_{S0})T_s \\ V_2, & (1-d_{S0})T_s<t<d_{S2}T_s \\ 0, & d_{S2}T_s<t<T_s \end{cases} \tag{2.2}$$

$$v_{L3}(t)=\begin{cases} V_3-V_0, & 0<t<(1-d_{S0})T_s \\ V_3, & (1-d_{S0})T_s<t<d_{S3}T_s \\ 0, & d_{S3}T_s<t<T_s \end{cases} \tag{2.3}$$

By applying inductor volt-second balance to (2.1)-(2.3), the relationship between source voltages, output voltage and duty cycles can be found as in (2.4).

$$\frac{V_1 d_{S1}}{(1-d_{S0})}=\frac{V_2 d_{S2}}{(1-d_{S0})}=\frac{V_3 d_{S3}}{(1-d_{S0})}=V_0 \tag{2.4}$$

Based on (2.4), one can notice that the d_{S1}, d_{S2} and d_{S3} meet an equilibrium point according to source voltages as given in (2.5).

$$V_1 d_{S1}=V_2 d_{S2}=V_3 d_{S3} \tag{2.5}$$

2.2. Mode1B

In Mode1B, Source-1 and Source-2 discharge to compensate load demand and to charge Source-3. Hence, i_{L1} and i_{L2} are positive while i_{L3} is negative. Additionally, the state of S_3 is unimportant in this mode so it is assumed that it is always OFF. This mode includes four switching subintervals as given in Figure 2.2b.

Subinterval 1 [$0<t<d_{s1}T_s$]: In this subinterval, the voltage and current variations of L_1 and L_2 are same with the ones in the first subinterval in Mode1A. On the other hand, due to the negative voltage across L_3, it is charged by positive i_{L1} and i_{L2} so its current is decreasing (increasing negatively). Moreover, since S_0 is not conducting, the output capacitor is also charged by L_1 and L_2.
Subinterval 2 [$d_{s1}T_s<t<(1-d_{s0})T_s$]: Like in the previous subinterval, in this subinterval, same voltage and current variations of L_1 and L_2 take place with the ones in the Subinterval 2 in Mode1A. Additionally, i_{L3} is still decreasing and the output capacitor current is still positive.
Subinterval 3 [$(1- d_{s0}) T_s <t< d_{s2}T_s$]: At $t=(1- d_{s0}) T_s$, this subinterval starts by closing S_0. i_{L1} is decreasing while i_{L2} is increasing as in the third subinterval in Mode1A. Because of the positive voltage across L_3, its current starts to increase (decrease negatively). The output capacitor starts to discharge for compensating load demand.
Subinterval 4 [$d_{s2}T_s<t<T_s$]: The last switching subinterval is initiated by turning OFF S_2. i_{L2} also becomes constant i_{L3} and the i_C maintain their trend in the previous subinterval.
The inductor voltage variations in Mode1B can be written as follows:

$$v_{L1}(t)=\begin{cases} V_1-V_0, & 0<t<d_{S1}T_s \\ -V_0, & d_{S1}T<t<(1-d_{S0})T_s \\ 0, & (1-d_{S0})T_s<t<T_s \end{cases} \tag{2.6}$$

$$v_{L2}(t)=\begin{cases} V_2-V_0, & 0<t<(1-d_{S0})T_s \\ V_2, & (1-d_{S0})T_s<t<d_{S2}T_s \\ 0, & d_{S2}T_s<t<T_s \end{cases} \tag{2.7}$$

$$v_{L3}(t)=\begin{cases} V_3-V_0, & 0<t<(1-d_{S0})T_s \\ V_3 & (1-d_{S0})T_s<t<T_s \end{cases} \tag{2.8}$$

By applying inductor volt-second balance to (2.6)-(2.8), the following relationship can be obtained.

$$\frac{V_1 d_{S1}}{(1-d_{S0})}=\frac{V_2 d_{S2}}{(1-d_{S0})}=\frac{V_3}{(1-d_{S0})}=V_0 \tag{2.9}$$

Based on source voltages, d_{S1} and d_{S2} change as given in (2.10).

$$V_1 d_{S1}=V_2 d_{S2}=V_3 \tag{2.10}$$

2.3. Mode2A

In this mode, regenerative braking energy is stored into Source-2 and Source-3; unlike these sources, Source-1 is not charged since the converter operates only in buck mode when storing regenerative braking energy. Thus, i_{L2} and i_{L3} are negative. L_2 automatically operates in discontinues conduction mode (DCM) because of the reason that will be explored later on. Moreover, i_{L1} is zero because the reference power of Source-1 is also zero. Mode 2A has three switching subintervals as shown in Figure 2.3a.
Subinterval 1 [$0<t<d_{T0}T_s$]: In this period, T_0 conducts therefore regenerative braking energy is transferred to the sources. The inductor voltages are negative and their currents are decreasing. The current of the output capacitor is also negative since it is discharged.
Subinterval 2 [$d_{T0}T_s<t<d_{\delta}T_s$]: At $t=d_{T0}T_s$, T_0 is turned OFF and i_{L2} reaches its peak value. Due to the positive voltage across L_2 and L_3, they start to discharge so their currents are decreasing. Furthermore, i_C becomes positive as regenerative braking energy charges the capacitor.
Subinterval 3 [$d_{\delta}T_s<t<T_s$]: This subinterval starts when i_{L2} becomes zero at $t= d_{\delta}$. Moreover, i_{L3} is still decreasing and i_C is still positive.

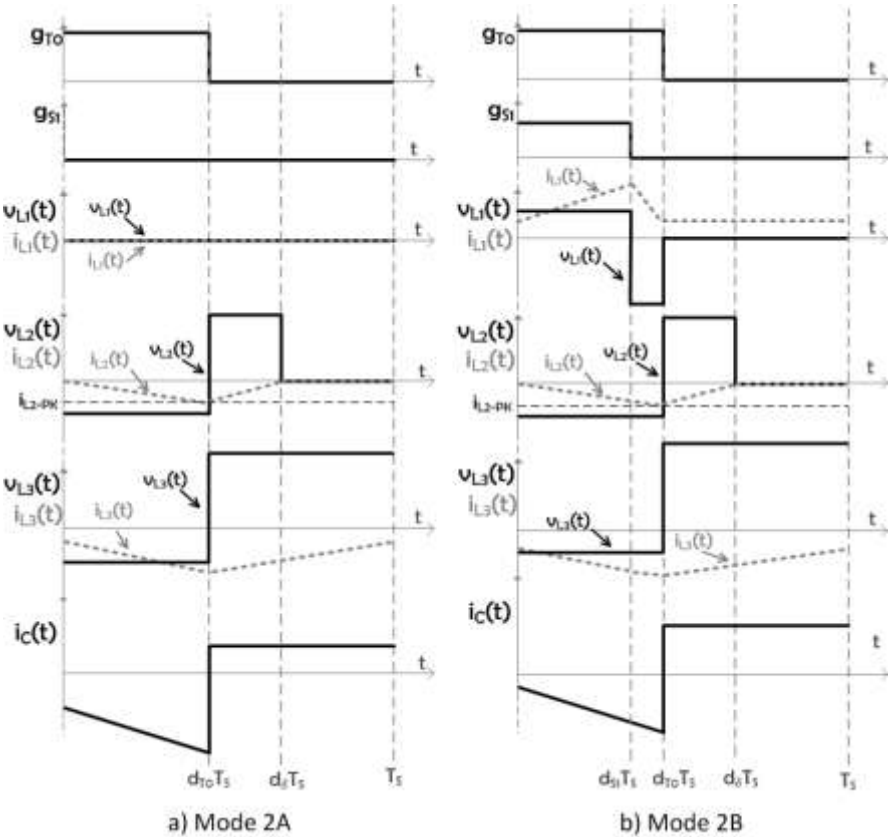

Figure 2.3. Waveforms for Mode 2A and Mode 2B. (Mode 2A ve Mode 2B için dalga şekileri)

The inductor voltages for these three subintervals can be given as follows.

$$v_{L2}(t)=\begin{cases} V_2-V_0, & 0<t<d_{S0}T_s \\ V_2, & d_{S0}T_s<t<d_\delta T_s \\ 0, & d_\delta T_s<t<T_s \end{cases} \tag{2.11}$$

$$v_{L3}(t)=\begin{cases} V_3-V_0, & 0<t<d_{T0}T_s \\ V_3 & d_{T0}T_s<t<T_s \end{cases} \tag{2.12}$$

By applying inductor volt-second balance to (2.12), the output voltage equation depending on V_3 and d_{T0} can be found as given in (2.13).

$$\frac{V_3}{d_{T0}}=V_0 \tag{2.13}$$

Peak value of i_{L2} can be easily calculated by examining Subinterval 1 or Subinterval 2. Since i_{L2} has constant slopes in these periods, the following equation can be written.

$$\left|i_{L2-PK}\right|=\frac{(V_0-V_2)}{L_2}\frac{d_{T0}}{f_S}=\frac{V_2}{L_2}\frac{d_\delta}{f_S} \tag{2.14}$$

According to (2.14), one can deduce that greater difference between V_0 and V_2 results in greater i_{L2} peak. In addition, increasing switching frequency, denoted by f_s, decreases the peak value of i_{L2}.

$$d_\delta=\frac{(V_0-V_2)}{V_2}d_{T0}=\frac{(V_0-V_2)}{V_2}\frac{V_3}{V_0} \tag{2.15}$$

In order to proof that L_2 works in DCM due to the assumed source voltage levels, let d_δ be equal to 1-d_{T0} and solve (2.15). As given in (2.16), in this case, voltage level of Source 2 and Source 3 should be equal.

$$V_2 = V_3, \text{ for } d_\delta = 1 - d_{T0} \tag{2.16}$$

From (2.16) one can see that if V_2 is greater than V_3, d_δ becomes lesser than 1-d_{T0} therefore i_{L2} reaches to zero before the end of the switching cycle; in other words, L_2 works in DCM.
Finally, average values of inductor currents can be calculated as in the following equations where P_{out} is the output power.

$$\left|i_{L2-av}\right| = \frac{\left|i_{L2-PK}\right|}{2}\left(d_{T0} + d_\delta\right) \tag{2.17}$$

$$\left|i_{L3-av}\right| = \frac{\left|P_{out}\right| - V_2\left|i_{L2-av}\right|}{V_3} \tag{2.18}$$

2.4. Mode2B

By recovering the regenerative braking energy, the studied converter can also enable energy transfer from the Source 1 to other two sources. This mode is quite useful to prevent sources from being overcharged/overdischarged and to store available renewable energy, such as solar energy. As shown in Figure 2.3b, i_{L1} is positive while i_{L2} and i_{L3} are negative in this mode, and i_{L3} still works in DCM. There are four different switching subintervals associated with this mode as analyzed below.

Subinterval 1 [$0<t<d_{S1}T_s$]: In this period, both d_{S1} and d_{T0} are conducting. All inductors are charged and the output capacitor is discharged.

Subinterval 2 [$d_{S1}T_s<t<d_{T0}T_s$]: At $t=d_{S1}$, S_1 is turned OFF and i_{L1} starts to decrease since the voltage across L1 becomes negative. Moreover, i_{L2}, i_{L3}, and i_C continue to decrease as in Subinterval 1.

Subinterval 3 [$d_{T0}T_s<t<d_\delta T_s$]: By opening T_0 at $t=d_{T0}$, the body diode of S_0 starts to conduct therefore the voltage of the inductor coupling point becomes zero. i_{L1} becomes constant since voltage of L_1 is zero and i_{L2} and i_{L3} starts to increase due to positive voltage across inductors. Furthermore, i_C is positive due to the regenerative braking energy.

Subinterval 4 [$d_\delta T_s<t<T_s$]: At $=d_\delta$, i_{L2} becomes zero and this subinterval starts. i_{L3} is still decreasing and i_{L1} is still constant. Moreover, the output capacitor goes on to be charged.

The inductor voltages variations for Mode 2B can be written as follows.

$$v_{L1}(t) = \begin{cases} V_1 - V_0, & 0 < t < d_{S1}T_s \\ -V_0, & d_{S1}T_s < t < d_{T0}T_s \\ 0, & d_{T0}T_s < t < T_s \end{cases} \tag{2.19}$$

$$v_{L2}(t) = \begin{cases} V_2 - V_0, & 0 < t < d_{S0}T_s \\ V_2, & d_{S0}T_s < t < d_\delta T_s \\ 0, & d_\delta T_s < t < T_s \end{cases} \tag{2.20}$$

$$v_{L3}(t) = \begin{cases} V_3 - V_0, & 0 < t < d_{T0}T_s \\ V_3 & d_{T0}T_s < t < T_s \end{cases} \tag{2.21}$$

According to inductor volt-second balance, by utilizing (2.19) and (2.20), the relationship between the output voltage, source voltages and duty cycles can be found as in (2.22).

$$\frac{V_3}{d_{T0}} = \frac{V_1 d_{S1}}{d_{T0}} = V_0 \tag{2.22}$$

From (2.22), it can be seen that in order to charge Source-3 by Source-1, V_1 should be higher than V_3 as expected. In this mode, the average of i_{L2} can be calculated as in Mode 2A by (2.17). Therefore, it does not change with the increasing i_{L1}. Finally, the average of i_{L3} can be calculated as below.

$$\left|i_{L3-av}\right| = \frac{\left|P_{out}\right| + V_1 i_{L1-av} - V_2 \left|i_{L2-av}\right|}{V_3} \tag{2.23}$$

3. FINDINGS (BULGULAR)

Although a switching model does not allow long time simulations due to the computational burden, it allows simulating power electronic converters in a great accuracy. Therefore, in order to test the converter, a switching model is created in PSIM environment.

Table 3.1. Simulation parameters. (Simülasyon parametreleri)

V_0*	100V
V_1	120V
V_2	90V
V_3	60V
L_1=L_2=L_3	150µH
C_0	2000µF
f_s	20kHz

In the simulation model, metal-oxide-semiconductor-field-effect-transistors (MOSFETs) are controlled by pulse-witdh-modulation (PWM) controllers. A load profile that represents propulsion and regenerative braking instants of an electric vehicle lasting 8-seconds is determined. Like in the analysis, in the simulation it is assumed that $V_1>V_0>V_2>V_3$. All simulation parameters are given in Table 3.1. Proposed control strategy for this work is illustrated in Figure 3.1. According to this figure, if the output power, P_o, is greater than zero, two PI controllers adjust d_{S1} and d_{S2} to control power levels of Source-1 and Source-2. Then, after deciding Mode1A or Mode1B is necessary, another PI controller controls d_{S3} or d_{S0} to transfer energy from/to Source-3. In Mode1A d_{S0} is kept at 0.5 for control simplicity. If P_0 is lower than zero, in other words, in the existence of regenerative braking energy, d_{T0} is adjusted for output voltage regulation while d_{S0} is always OFF. In this case, P_1 is regulated its reference value through a PI controller that controls d_{S1}. Since this work mainly focuses on the analysis of the converter and operation modes, it is not targeted to propose an optimum control strategy. Therefore, reference values of source power levels are determined arbitrarily: reference of P_1 is assumed to be 300W between 0~4s and 100W between 5s~7s; moreover, reference of P_2 is calculated to provide extra power on condition that it does not exceed 500W.

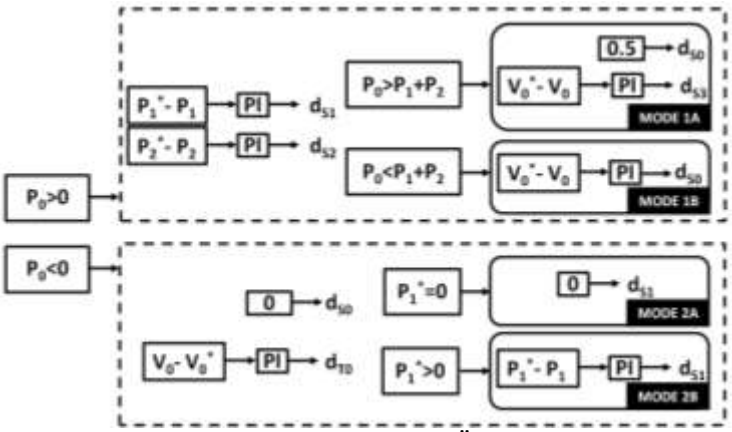

Figure 3.1. Proposed control strategy. (Önerilen kontrol yöntemi)

Figures 3.2-3.4 show simulation results. In Figure 3.2a, variation of output power is given. As can be seen here, it is varied between 1000W and -500W with different rising and falling slopes.

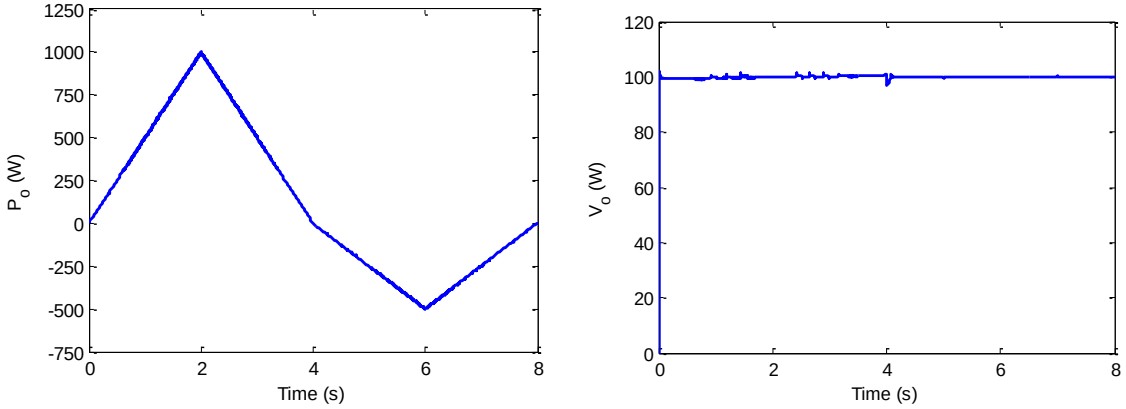

(a) (b)

Figure 3.2. a) Output power (Çıkış gücü), b) Output voltage (Çıkış gerilimi)

In Figure 3.2b, the output voltage is given. From this figure, one can see that it is successfully regulated at 100V despite of varied output power and varied source power levels as highlighted below.

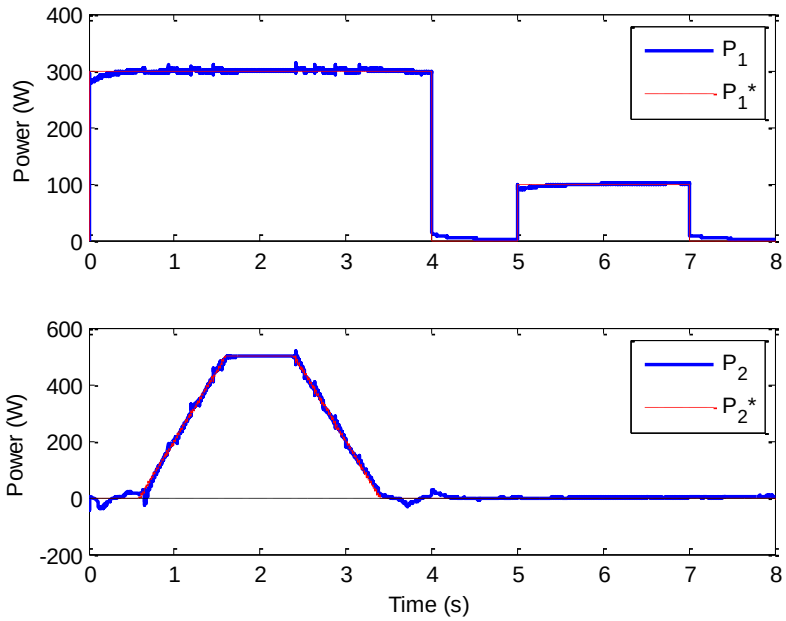

Figure 3.3. Power levels and power references of Source-1 and Source-2. (Kaynak-1 ve Kaynak-2'nin güç seviyeleri ve güç referansları)

From Figure 3.3 that demonstrate power levels and power references of Source-1 and Source-2. As seen, even though PI controllers in the simulation model are not optimized, power level of sources well follow their reference values when the output power is positive or negative.

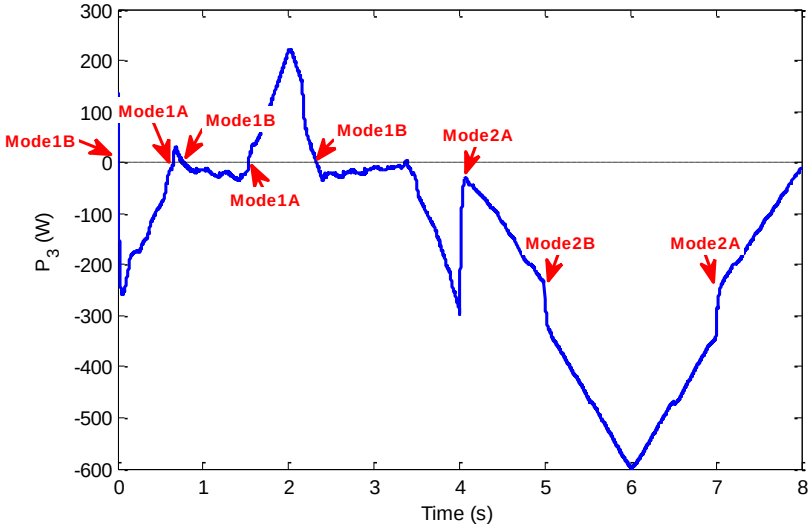

Figure 3.4. Power levels of Source-3 and mode transition points. (Kaynak-3'ün güç seviyesi ve mod değişim noktaları)

Finally, Figure 3.4 shows the variations in P_3 and mode transition instants. In the beginning of the simulation, since total power of other sources are higher than the output power, the converter works in Mode1B and charge Source-3 as can be deduced from its negative power. By the increment in the output power, Source-3 starts to discharge in Mode1A. After 4s, the converter changes its mode to Mode2A, and transfers regenerative braking energy to Source-3. At 5th second, P_1 increases from zero to 100 as can be seen in Figure 3.3. At that moment, P_3 decreases (increases negatively) sharply and converter mode becomes Mode2B since Source-1 also charges Source-3.

4. CONCLUSION AND DISCUSSION (SONUÇ VE TARTIŞMA)

In this paper, a bidirectional multi-input converter dc-dc converter for 3-input case has been analyzed. This converter can be utilized to construct hybrid systems for electric vehicles that may include different energy storage elements, such as, batteries, UCs, and alternative energy sources, such as, PVs, FCs; by this kind of hybridization, it can eliminate their drawbacks and gather their powerful features. Four different operation modes of the converter have been introduced; typical waveform for these modes has been given. After that, equations as functions of source voltages, output voltage, and duty cycles for each mode have been derived. Finally, a switching simulation model has been created and dynamic performance of the converter has been tested. According to test results, it has been seen that the converter can enable power sharing between sources as expected and mode transitions are realized properly.

5. REFERENCES (KAYNAKLAR)

[1] Khaligh, A. (2010). Battery, Ultracapacitor, Fuel Cell, and Hybrid Energy Storage Systems for Electric, Hybrid Electric, Fuel Cell, and Plug-In Hybrid Electric Vehicles: State of the Art, *IEEE Transactions Vehicular Technology*, 59(6), 2806–2814.

[2] Chan, C. C. (2002). The state of the art of electric and hybrid vehicles. *IEEE Conference on Computer Security Application*, Washington, 245-275.

[3] Lukic, S. M., Bansal, R. C., Rodriguez, F., and Emadi, A. (2008). Energy Storage Systems for Automotive Applications, *IEEE Transactions on Industrial Electronics*, 55(6), 2258–2267.

[4] Erdinc, O., Vural, B., Uzunoglu, M. (2009). A wavelet-fuzzy logic based energy management strategy for a fuel cell/battery/ultracapacitor hybrid vehicular power system, *Journal of Power Sources*, 194(1), 369-380.

[5] Nejabatkhah, F., Danyali, S., Hosseini, S. H., Sabahi, M., and Niapour, S. M. (2012). Modeling and control of a new three-input dc-dc boost converter for hybrid PV/FC/battery power system. *IEEE Transactions on Power Electronics*, 27(5), 2309–2324.

[6] Akar F., and Vural, B. (2013). Battery/UC hybridization for electric vehicles via a novel double input DC/DC power converter, *3rd International Conference on Electric Power and Energy Conversion Systems*, Istanbul, 1–4.

[7] Akar, F., Tavlasoglu, Y., Ugur, E., Vural, B., and Aksoy, I. A bidirectional non-isolated multi input DC-DC converter for hybrid energy storage systems in electric vehicles, *IEEE Transactions on Vehicular Technology*, PP(99).

[8] Özdemir, E., Çalıker, A., and Koç, İ. M. (2014). Yenilenebilir Enerji Kaynağından Beslenen Elektrik Güç Sistemleri İçin Hibrit Enerji Depolama Teknolojileri. *International Energy&Environment Fair&Conference*, Istanbul, 1-5.

[9] Vural,B., Erdinc, O., Uzunoglu, M. (2010). Parallel combination of FC and UC for vehicular power systems using a multi-input converter-based power interface, *Energy Conversion and Management*, 51(12), 2613-2622.

[10] Jianming, X., Kang, L., and Zhang, Y. (2011). Design of a hybrid PV/UC/batteries system, *IEEE International Conference on Cyber Technology in Automation, Control, and Intelligent Systems*, Kunming, 57-61.

[11] Schaltz, E., Khaligh A., and Rasmussen, P. O. (2008). Investigation of battery/ultracapacitor energy storage rating for a fuel cell hybrid electric vehicle, *Vehicle Power and Propulsion Conference*, Harbin, 1-6.